RESEARCH PROGRESS IN MECHANICAL AND MANUFACTURING ENGINEERING
e-ISSN: 2773-4765

RPMME

Vol. 5 No. 2 (2024) 252-263
https://publisher.uthm.edu.my/periodicals/index.php/rpmme

Development and Testing of a Test Rig for Coaxial Motor-Propeller Configurations

Wong Qi En[1], Wan Saiful-Islam Wan Salim[1]*

[1] *Department of Mechanical Engineering, Faculty of Mechanical and Manufacturing Engineering, Universiti Tun Hussein Onn Malaysia, Parit Raja, 86400, Johor, MALAYSIA*

*Corresponding Author: wsaiful@uthm.edu.my
DOI: https://doi.org/10.30880/rpmme.2024.05.02.028

Article Info

Received: 21 May 2024
Accepted: 20 August 2024
Available online: 31 December 2024

Keywords

UAVs, eVTOL, Coaxial Motor-Propeller Test Rig, Configurable Mounting Bracket, Varying Propeller Distance and Tilt Angle, Thrust

Abstract

This study focuses on the development and testing of a versatile test rig designed to evaluate coaxial motor-propeller systems, which is crucial for UAVs and eVTOL aircraft designs. The rig includes a configurable mounting bracket assembly, connecting arms, an aluminium support frame, and accurately placed load cells, all connected via a universal mounting platform. The bespoke key components were specifically designed and fabricated for durability and weight reduction while providing stability during tests. The tests were carried out by varying propeller distance and tilt angle at different motor speeds to assess their impact on thrust. Findings indicate that increasing the distance between propellers initially boosts thrust, peaking at a 12 cm coaxial distance, after which thrust decreases due to diminished aerodynamic effectiveness. Increasing the tilt angle consistently enhances thrust, demonstrating its critical role in optimising performance. The results underscore that while both parameters are important, adjusting the tilt angle significantly improves thrust more than distance variations. This insight is valuable for designing efficient coaxial systems. Future research should further investigate the combined effects of distance and tilt angle to enhance system efficiency in aerospace applications.

1. Introduction

In the rapidly evolving field of aerospace engineering, the optimisation of motor-propeller systems is paramount, particularly in the context of Unmanned Aerial Vehicles (UAVs) and Electric Vertical Take-Off and Landing (eVTOL) aircraft. These technologies demand compact, efficient systems capable of maximising thrust while minimising size and weight. Coaxial motor-propeller configurations featuring stacked propellers rotating in opposite directions on a single axis present a promising solution due to their potential for enhanced thrust and streamlined design. However, understanding how variations in configuration parameters, such as the distance between propellers and their tilt angles, impact performance remains a significant challenge. Despite the recognised benefits of coaxial systems in reducing overall size and improving aerodynamic efficiency, comprehensive analyses of how different configurations affect their performance are limited (1).

Addressing this knowledge gap is critical for applications where space constraints and high thrust efficiency are crucial, such as in UAVs and eVTOLs for urban air mobility (2). This study aims to tackle this issue by developing a versatile and adjustable test rig capable of accurately measuring the performance of coaxial motor-propeller systems under various configurations. The research focuses on experimentally investigating the effects of different distances and tilt angles between propellers on thrust production. Achieving these objectives will provide valuable insights into optimising coaxial systems for improved aerodynamic performance (3).

The significance of this research extends beyond theoretical analysis, offering practical contributions to the field of aerospace engineering. The study enhances the foundational understanding necessary for designing and optimising these systems by detailing how configuration changes impact coaxial motor-propeller systems. The results of this investigation could directly influence the development of more efficient UAVs and eVTOL aircraft, which are becoming increasingly essential for both commercial and personal use (4). Additionally, the test rig developed through this study will be a valuable tool for further research and development, facilitating the exploration of other parameters and configurations.

The theoretical background for this study is rooted in the dynamics of coaxial rotor systems. These systems, which utilise two rotors spinning in opposite directions on a single axis, are known for their potential to increase thrust efficiency while maintaining a compact design. This configuration helps cancel out the rotational torque generated by each rotor, thereby improving stability and reducing energy loss (1). However, the aerodynamic interaction between the rotors can lead to complex phenomena that need to be carefully managed to optimise performance. Understanding these interactions is crucial for leveraging the advantages of coaxial designs in practical applications (5).

In summary, this study aims to fill the current gap in knowledge regarding the optimisation of coaxial motor-propeller systems by exploring the effects of propeller distance and tilt angle on thrust performance. The insights gained from this research will be vital for advancing UAVs and eVTOL aircraft, offering pathways to more efficient and effective designs.

2. Methodology

The flow chart in Fig.1 outlines a detailed process and various stages of the design and testing of a test rig. It encompasses identifying measurement parameters, clarifying the rig's function, selecting materials and components, designing the main frame and a configurable motor mounting plate, and determining the test rig's size. Following the assembly sketching, the process evaluates the design's satisfaction. If the objective is achieved, data analysis takes place, leading to a conclusion. The process returns to the design phase if the objective is not met. The process culminates after successful testing and data analysis.

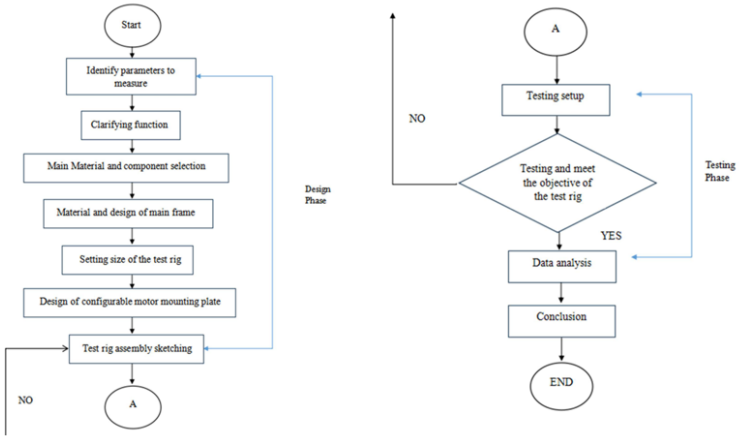

Fig 1. *Flow chart of the work activities*

2.1 Test Rig Design

In the design phase of this study, the focus was on creating a robust and versatile test rig capable of evaluating the performance of coaxial motor-propeller systems under varying configurations. The primary components of the rig included a configurable mounting bracket assembly, connecting arms, an aluminium support frame, and precisely positioned load cells for accurate thrust measurement. These components were interconnected via a universal mounting platform, allowing for adjustable positioning of the motor-propeller units.

To ensure structural integrity and adaptability, complex assembly parts were manufactured using 3D-printed PETG, known for its lightweight and durable properties. Aluminium profiles were selected for the support frame to provide strength and stability. This design choice facilitated ease of modification, enabling precise adjustments to the distance and tilt angles between the propellers. The design process emphasises modularity and precision, which are crucial for replicating the aerodynamic conditions in actual UAV and eVTOL applications (6).

2.1.1 Design Requirements

An objective tree is constructed after acknowledging that thrust is the main variable the test rig will be measuring. An objective tree for the test rig development would be a hierarchical representation of the main objectives and sub-objectives related to creating and utilising the specialised test rig for evaluating coaxial motor-propeller configurations. The main objective, often depicted at the top of the tree, would be to design, fabricate, test, and calibrate the test rig to ensure its reliability and accuracy in evaluating coaxial motor-propeller configurations. The objective tree diagram for the test rig is shown in Fig. 2 below.

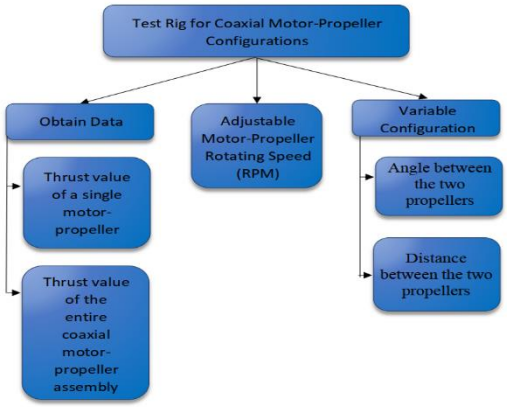

Fig. 2 *Objective Tree Diagram of the Test Rig*

2.1.2 Main Components and Functions

In the process of clarifying the function of the test rig for evaluating coaxial motor-propeller configurations, the initial step involves Component Decomposition Analysis. This entails breaking down the test rig into its fundamental components to understand their distinct functions. The component decomposition analysis involves a detailed breakdown of the constituent parts and sub-assemblies. This breakdown is represented in a hierarchical structure of component forms, focusing on the physical composition rather than functional aspects. This analysis aimed at gaining a thorough understanding of how individual components within the test rig interact and contribute to its overall functionality. Fig. 3 below shows the component decomposition diagram of the test rig for coaxial motor-propeller configurations.

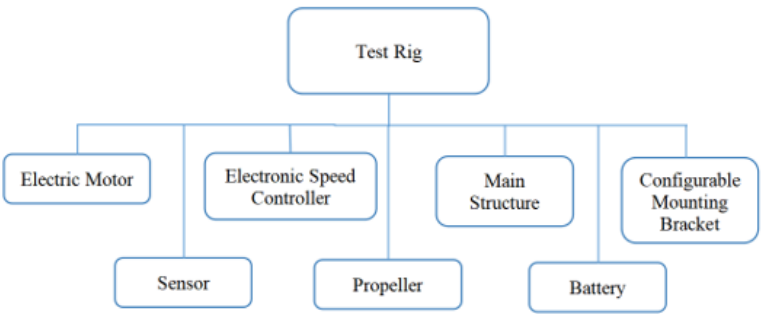

Fig. 3 *Component Decomposition of the Test Rig*

Fig. 4 shows the function decomposition analysis of the specialised test rig for evaluating coaxial motor-propeller configurations. Each component is shown to fulfil its designated role within the system. Moreover, the illustration highlights the close functional connection between the main component and the subcomponents, enabling the system to maintain optimal conditions and operate continuously in a cycle.

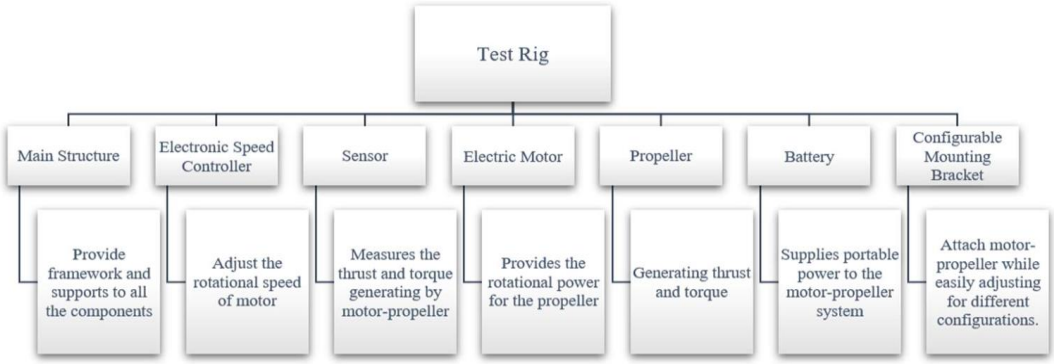

Fig. 4 *Function Decomposition Analysis*

2.1.3 Morphological Chart

The morphological chart, as shown in Table 1, is a powerful visual aid in engineering, design, and problem-solving, offering a systematic framework for exploring and generating potential solutions to the intricate challenges posed by coaxial motor-propeller configurations. This method uses a structured approach to deconstruct the problem, breaking it into its core components or parameters. Each row within the chart corresponds to a specific aspect or parameter, while each column delineates the various options or possibilities within that aspect. Notably, the chart exhibits several choices and alternatives for all the main components of the test rig, including the main structure, motor, sensor, electronic speed controller (ESC), propeller, configurable mounting bracket, and battery. This comprehensive representation allows for a versatile selection from a range of component types.

In dealing with multidimensional problems, where numerous factors and parameters come into play, morphological charts provide an organised platform for brainstorming. Systematic exploration enables the generation of innovative solutions by considering diverse combinations of variables. As embark on the development and testing of a test rig tailored for coaxial motor-propeller configurations, the morphological chart proves indispensable. It facilitates a structured and comprehensive approach to problem-solving and design exploration, offering a multitude of choices and alternatives for each critical component of the test rig.

Table 1 *Morphological Chart of the Test Rig*

Component	Alternative 1	Alternative 2	Alternative 3
Main structure	Aluminium profile	Stainless steel bar	3D printing
Electronic Speed Controller (ESC)	Brushed ESC	Brushless ESC	2 in-1 ESC
Sensor	Load cells	Thin-film force sensor	Thrust and torque sensor
Electric Motor	Brushless DC motor	Brushed DC motor	Coreless motor
Propeller	8x4 (inch)	5x3 (inch)	4.2x4 (inch)
Battery	Lithium Polymer (LiPo) battery	Lithium Ion (Li-ion) battery	Nickel-metal hydride (NiMH) battery
Configurable Mounting Bracket	3D Printing	Aluminium	Carbon Fiber

2.1.4 Layout of Test Rig

Fig. 5 shows the test rig assembly sketching, including some important components of the test rig, such as the BLDC motor, propeller, load cells for thrust, configurable mounting plate, arm, pivot, and main support frame created by aluminium profiles.

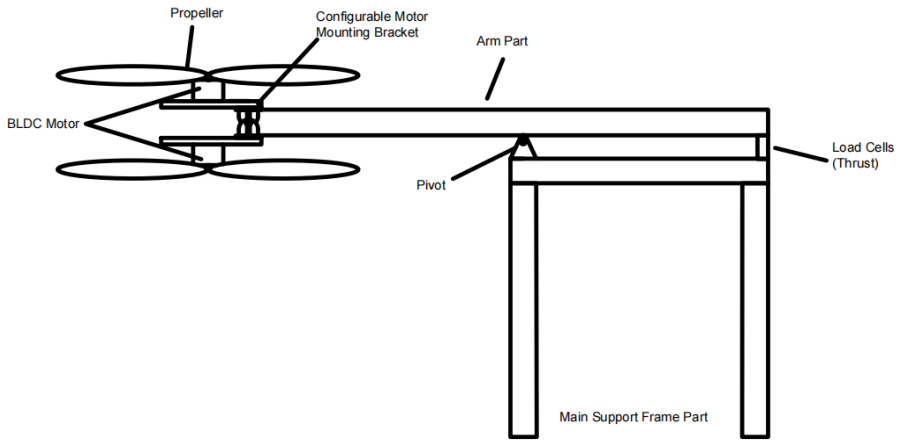

Fig.5 *Schemtic illustration of the test rig*

The design of a configurable motor mounting bracket is essential for the versatility and adaptability of the test rig. This specialised component allows for dynamic adjustment of the distance between the two motor-propeller units and the angle between them. The capability to modify these parameters is crucial for exploring a wide range of coaxial motor-propeller configurations. Fig. 6(a) shows the engineering drawing of it, enabling the alteration of the distance between the motors and facilitating precise control over the spatial arrangement. This adjustability is essential for assessing the impact of different motor-propeller spacings on the overall aerodynamic performance of the coaxial configuration. Similarly, Fig. 6(b) illustrates the design for adjusting the angle between the two motor-propellers. This feature is instrumental in exploring the aerodynamic effects resulting from variations in the angle of incidence. The ability to configure both the distance and angle provide a comprehensive platform for experimental investigations, enabling a nuanced understanding of coaxial motor-propeller interactions.

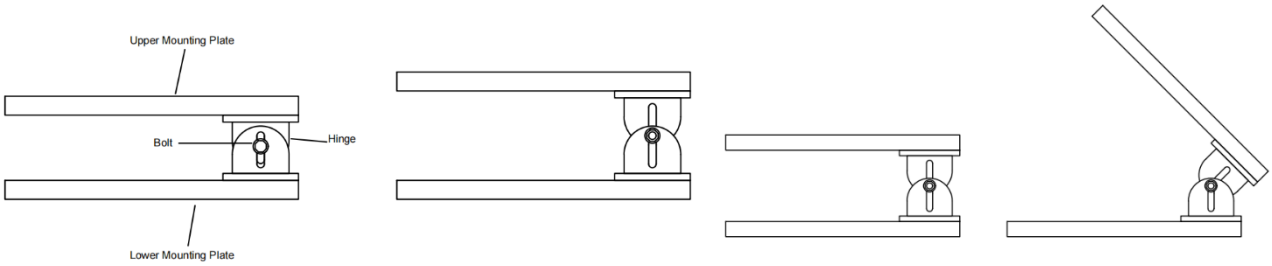

Fig.6 *(a) Adjustable Distance Between Two Motor-Propeller, (b) Adjustable Angle Between Two Motor-Propeller*

2.2 Testing Phase

The step-by-step procedure is designed to ensure the testing runs smoothly and systematically, contributing to understanding coaxial motor-propeller configurations. The experiment procedures are shown below:

- The first step is to verify the correct setup and optimal condition of all components in the test rig by meticulously verifying each component's functionality and the system's overall integrity.
- The experiment is initiated by starting the motor-propeller system and gradually adjusting the RPM speed of the motor. This step allows for a systematic exploration of the system's performance across different speed settings, with the recommendation to increment the RPM gradually for nuanced observations.
- Simultaneously, data collection of the experiment outcomes is conducted for each motor-propeller speed using the Arduino IDE software. Precise data collection is crucial for subsequent analysis and interpretation, ensuring the reliability and robustness of the experimental results.
- The experiment's scope is then expanded by modifying coaxial motor-propeller configurations. This involves changing the angle between the two propellers, and adjusting the distance between the propellers
- Each configuration change is systematically tested by repeating the experiment steps, ensuring a thorough exploration of the coaxial motor-propeller system's behavior under diverse settings.

The test rig for coaxial motor-propeller configurations will be set as the Fig. 7.

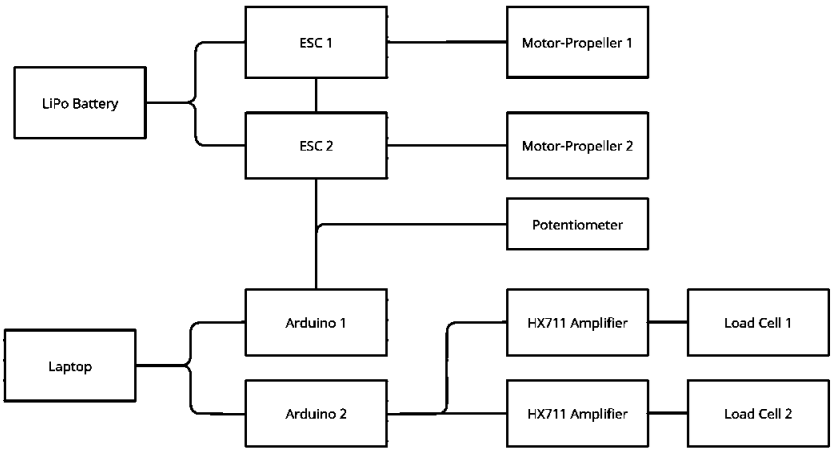

Fig.7 *Test Rig Block Diagram*

Electric motors play a pivotal role in converting electrical energy into mechanical motion within electromechanical systems. These systems are defined by specific parameters such as torque, current, and voltage, which can be precisely acquired using a dyno and a power analyser. The 8x4 drone propeller, featuring an 8-inch diameter and 4-inch pitch, was selected for the coaxial motor-propeller configuration test rig due to its balanced characteristics. Next, the selection of an ESC (Electronic Speed Controller) hinges on its ability to handle the peak current of the motor. In our experiment, where the motor is not expected to draw more than 30 A, the chosen ESC is a suitable match. When choosing a battery for a drone, Lithium Polymer (LiPo) batteries are often preferred over Lithium-Ion batteries due to their lighter weight, rapid discharge rates, and versatile form factors. Fig. 8 below shows the main component of the test rig.

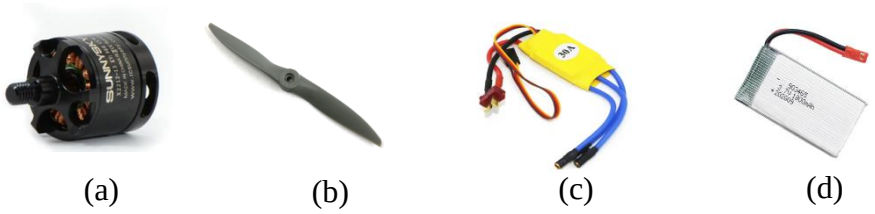

Fig. 8 Basic components of motor-propeller system: *(a) BLDC Motors; (b) 8x4 Propeller; (c) ESC; (d) LiPo Battery*

2.3 Data Analysis

The core of the data collection process involved using load cells connected to an Arduino microcontroller. This setup enabled continuous monitoring and recording of the thrust data. The Arduino was programmed to update and display the thrust readings every second, providing real-time insights into the forces generated by the system. This frequent data update ensured a comprehensive capture of the thrust variations over time, allowing for a detailed analysis.

For each RPM setting, starting from 3500 RPM and increasing in 500 RPM increments up to 6500 RPM, the system was allowed to stabilise to minimise transient effects. Once the system reached a steady operating state, thrust data was recorded every second over an extended period. This approach generated a large dataset, typically comprising thousands of individual readings for each RPM setting. The high frequency of data capture ensured that the subtle changes in thrust could be accurately tracked and analysed.

The collected data was then transferred from the Arduino to Microsoft Excel, chosen for its ease of access and sufficient data handling and visualisation capabilities. The thrust readings were plotted against RPM. These graphs provided a clear visual representation of how thrust varied over time. The graphical plots revealed distinct patterns, with initial fluctuations followed by periods of stable thrust readings. Identifying these stable periods was crucial as they indicated the system had reached a steady state, where the thrust produced by the propellers was consistent and reliable for analysis.

Within these stable regions on the graph, a subset of approximately one hundred readings was selected for each RPM setting. These selected readings represented the most consistent performance of the system, free from the initial transient fluctuations. By focusing on these stable readings, the accuracy of the analysis was significantly enhanced. To further ensure reliability, the selected readings were averaged to obtain a representative thrust

value for each RPM setting. This averaging process minimised the impact of minor fluctuations or noise in the data, providing a more accurate measure of the thrust generated by the system.

3. Results and Discussion

This section presents the detailed design of the coaxial motor-propeller test rig and discuss the results of the experiments conducted to evaluate the performance of various propeller configurations.

3.1 Final Design

The final configuration of the coaxial motor-propeller test rig assembly is shown in Fig. 9 below. The test rig's overall dimensions are approximately 1224 mm in height, 1278 mm in length, and 440 mm in width.

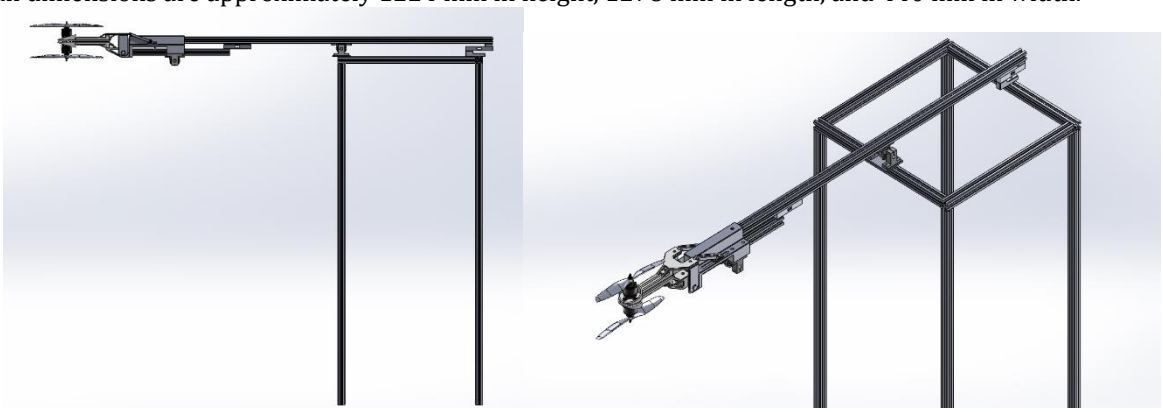

(a) **(b)**

Fig. 9 *(a) Side View of the Test Rig Assembly; (b) Isometric View of the Test Rig Assembly*

3.1.1 Design of Configurable Mounting Bracket Assembly

At the heart of the rig are the Brushless DC (BLDC) motors and propellers, as shown in Fig. 10, which generate the necessary thrust. These are securely mounted on an adjustable bracket that provides a range of alignment and positioning options, enabling the testing of various configurations. This bracket is crucial for holding the motor-propeller assemblies in place and enabling adjustments needed for experimental variations. Its design is both strong and flexible, accommodating the dynamic needs of testing multiple configurations.

Fig. 10 *Configurable Mounting Bracket*

The hinge is a critical component that connects the Universal Mounting Platform to the top motor-propeller mount in the coaxial motor-propeller test rig. This hinge enables the adjustment of both the tilting angle and the distance between the two motor-propeller units, as shown in Fig. 11. By allowing precise angular adjustments, the hinge enables the top motor-propeller to be tilted at various angles relative to the bottom unit. This flexibility is crucial for exploring how different tilting angles affect the aerodynamic performance and interaction of the coaxial propellers. Additionally, the hinge facilitates the adjustment of the vertical distance between the propellers, ensuring that the spacing can be finely tuned to suit various experimental setups.

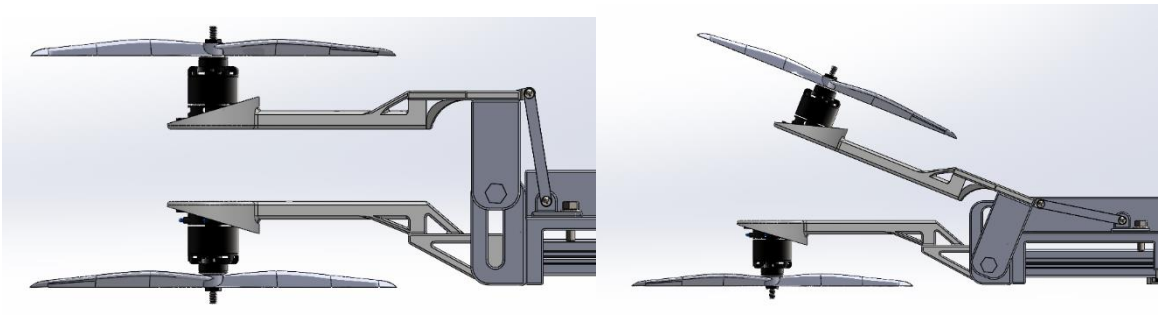

(a) **(b)**

Fig. 11 *(a) Adjustable Distance; (b) Adjustable Tilt Angle*

3.1.2 Load Cell Position and Spacer Plate

To capture the performance data, the test rig employs two types of load cells. *Load Cell 1* assesses the total thrust produced by the entire coaxial assembly, allowing for the evaluation of the combined effects and interactions between the propellers. The *Load Cell 2* measures the thrust generated by a single motor-propeller unit, providing insight into its individual performance. Pivot bearings play a pivotal role in the test rig by allowing for the smooth rotation and support of the motor-propeller assemblies. Positioned between the motor-propeller units and the load cells, the pivot bearings create a lever system as shown in Fig. 12. When the motor-propeller generates upward thrust, this force acts upward against the pivot bearing. Due to the nature of the pivot, a reaction force is produced downward, acting on the load cell. This setup effectively translates the thrust force into a measurable compressive force on the load cell.

Fig. 12 *Lever System of Test Rig*

To effectively measure the compressive force, the load cell must be able to deform slightly under load. This deformation changes the electrical resistance of the strain gauges within the load cell, converting the mechanical force into an electrical signal. For the load cell to deform properly, there must be sufficient clearance around it. This is achieved by placing spacer plates at both ends of the load cell, which is shown in the Fig. 13 below. These spacer plates ensure that the load cell is not fully constrained and can undergo the necessary deformation when a force is applied.

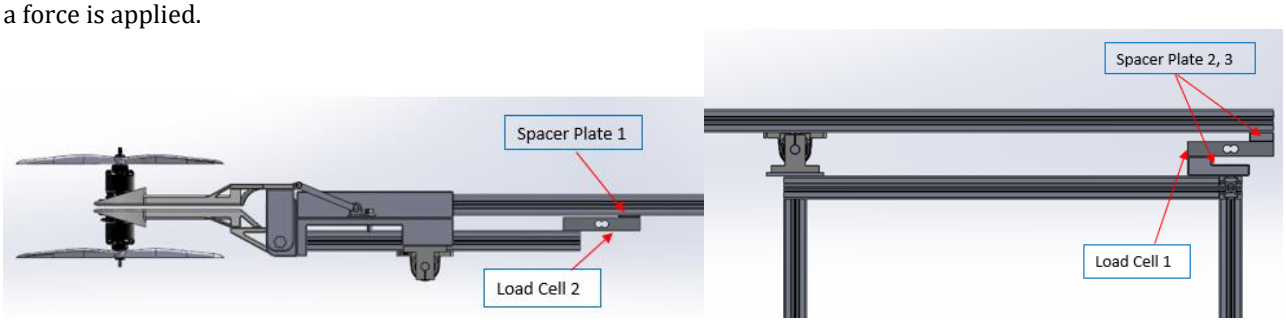

(a) **(b)**

Fig. 13 *(a) Spacer Plates 1 of Load Cell 2*; *(b) Spacer Plates 2, 3 of Load Cell 1*

3.2 Testing Results

This chapter will discuss the experimental results obtained from testing various configurations of the coaxial motor-propeller system. The analysis focuses on the thrust readings from two load cells under different conditions: varying the distance between the propellers and altering the tilt angle of the propellers. Load Cell 1 measures the thrust of the entire coaxial system, while Load Cell 2 measures the thrust from the bottom propeller.

3.2.1 Thrust Analysis with Varying Distance Between Propellers

From Table 2 and Fig. 14(a), we can observe a complex relationship between thrust and the distance between the propellers. At lower RPMs (3500-4500 RPM), the thrust generally increases with a slight increase in the distance, peaking around 11-12 cm, but decreases at 13 cm. For example, at 6000 RPM, the thrust reaches 5.193 N at 12 cm, then decreases slightly at 13 cm. This behaviour suggests that an optimal distance exists where the interaction effects between the propellers are minimised.

Table 2 *Thrust Reading from Load Cell 1 with Varying Distance Between Propellers*

Speed (RPM)	Thrust Reading from Load Cell 1 (N)			
	Distance Between Propellers (cm)			
	10	11	12	13
3500	2.086	2.169	2.224	2.098
4000	2.810	2.680	2.586	2.455
4500	3.574	3.017	2.989	2.985
5000	4.102	3.580	3.762	3.744
5500	4.470	4.294	4.411	4.387
6000	5.038	5.067	5.193	5.127
6500	5.961	5.982	6.158	5.995

The readings from Load Cell 2 in Table 3 also indicate an increase in thrust with increasing RPMs, but the impact of varying distances between the propellers is less pronounced compared to Load Cell 1. For instance, at 6500 RPM, the thrust varies minimally across different distances, ranging from 1.674 N at 10 cm to 1.585 N at 13 cm.

Table 3 *Thrust Reading from Load Cell 2 with Varying Distance Between Propellers*

Speed (RPM)	Thrust Reading from Load Cell 2 (N)			
	Distance Between Propellers (cm)			
	10	11	12	13
3500	0.236	0.289	0.386	0.327
4000	0.636	0.409	0.292	0.232
4500	1.064	0.388	0.297	0.435
5000	1.231	0.697	0.752	0.914
5500	1.192	1.045	1.022	1.157
6000	1.237	1.283	1.259	1.335
6500	1.674	1.614	1.560	1.585

The data in Table 4 shows that the thrust difference increases with RPM, highlighting the enhanced interaction at higher speeds. At 6500 RPM, the maximum thrust difference occurs at 12 cm which is 4.598 N. This reinforces the observation that a certain distance of around 12 cm optimises the thrust due to effective coaxial interaction. Fig. 14 shows the chart for thrust readings with varying distances between propellers.

Table 4 *Thrust Difference of Load Cell 1 and 2 with Varying Distance Between Propellers*

Speed (RPM)	Thrust Difference of Load Cell 1 and 2 (N)			
	Distance Between Propellers (cm)			
	10	11	12	13
3500	1.850	1.881	1.839	1.771
4000	2.174	2.271	2.294	2.223
4500	2.510	2.629	2.692	2.550
5000	2.871	2.883	3.010	2.830
5500	3.278	3.249	3.389	3.230
6000	3.801	3.784	3.934	3.792
6500	4.287	4.369	4.598	4.410

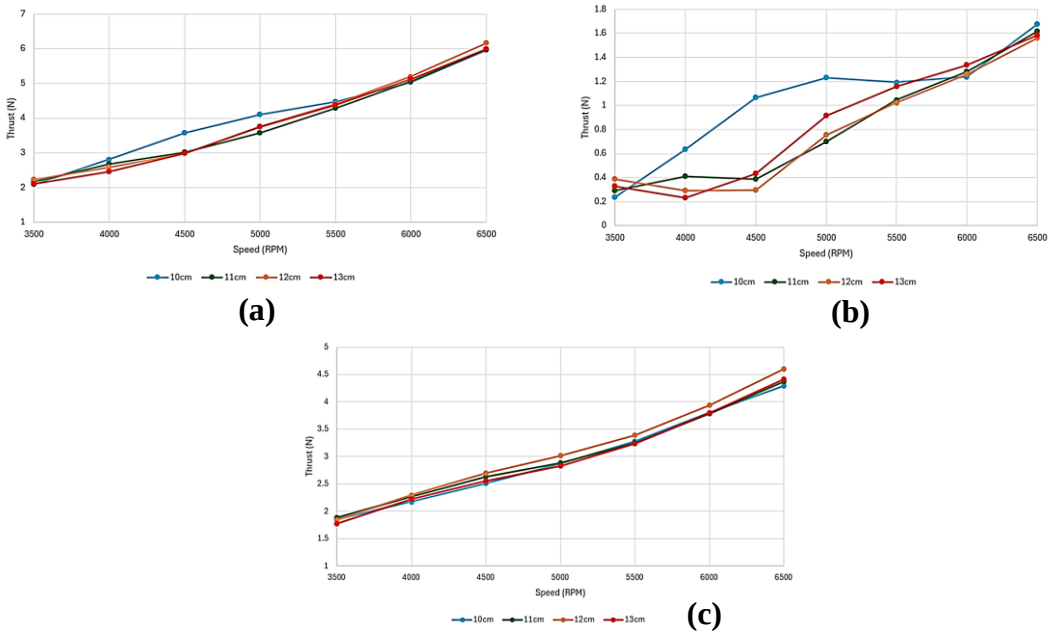

Fig. 14 *(a) Thrust Reading from Load Cell 1*; *(b) Thrust Reading from Load Cell 2; (c) Thrust Difference of Load Cell 1 and 2*

3.2.2 Thrust Analysis with Varying Tilt Angle of Propeller

The data in Table 5 below indicates a significant increase in thrust with increasing tilt angles, especially at higher RPMs. For example, at 6500 RPM, the thrust increases dramatically from 5.995 N at 0° to 7.376 N at 15°. This trend suggests that tilting the propellers enhances the system's aerodynamic efficiency, likely by reducing direct aerodynamic interference and optimising the airflow path. This increased thrust with larger tilt angles highlights the potential for tilt adjustments to significantly boost performance in coaxial propeller systems. It appears that the propeller tilt can mitigate some of the adverse effects of coaxial interference, leading to a more streamlined and efficient thrust production.

Table 5 *Thrust Reading from Load Cell 1 with Varying Tilt Angle of Propeller*

Speed (RPM)	Thrust Reading from Load Cell 1 (N)					
	Tilt Angle of Propellers (Degree)					
	0	6	8	10	13	15
3500	2.098	2.171	2.232	2.117	2.309	2.277
4000	2.455	2.914	2.936	2.748	3.128	3.134
4500	2.985	3.774	3.712	3.507	3.873	3.934
5000	3.744	4.565	4.421	4.112	4.563	4.715
5500	4.387	5.273	5.228	4.848	5.345	5.424
6000	5.127	6.017	6.094	5.682	6.118	6.207
6500	5.995	6.656	7.315	6.592	7.229	7.376

For the single motor-propeller, the thrust readings in Table 6 also show an increase with tilt angle, though the increases are less dramatic compared to the overall thrust measurements. At 6500 RPM, the thrust rises from 1.585 N at 0° to 2.010 N at 15°.

Table 6 *Thrust Reading from Load Cell 2 with Varying Tilt Angle of Propeller*

Speed (RPM)	Thrust Reading from Load Cell 2 (N)					
	Tilt Angle of Propellers (Degree)					
	0	6	8	10	13	15
3500	0.327	0.246	0.276	0.318	0.434	0.326
4000	0.232	0.606	0.580	0.603	0.809	0.662
4500	0.435	1.210	0.976	1.025	1.181	1.032

5000	0.914	1.643	1.326	1.271	1.357	1.273
5500	1.157	1.872	1.670	1.559	1.659	1.430
6000	1.335	2.106	2.002	1.893	1.942	1.629
6500	1.585	2.140	2.530	2.282	2.369	2.010

The thrust difference consistently increases with higher tilt angles, as shown in Table 7, suggesting that tilting enhances the interaction effects between the propellers. At 6500 RPM, the difference grows from 4.410 N at 0° to 5.367 N at 15°, demonstrating that greater tilt angles effectively amplify the coaxial benefits by improving the overall thrust production.

Table 7 *Thrust Difference of Load Cell 1 and 2 with Varying Tilt Angle of Propeller*

Speed (RPM)	Thrust Difference of Load Cell 1 and 2 (N)					
	Tilt Angle of Propellers (Degree)					
	0	6	8	10	13	15
3500	1.771	1.924	1.956	1.799	1.875	1.952
4000	2.223	2.308	2.356	2.145	2.320	2.472
4500	2.550	2.564	2.736	2.483	2.692	2.901
5000	2.830	2.922	3.095	2.841	3.206	3.442
5500	3.230	3.401	3.557	3.288	3.685	3.993
6000	3.792	3.911	4.092	3.789	4.176	4.578
6500	4.410	4.516	4.785	4.310	4.860	5.367

Fig. 15 below shows the chart for thrust readings with varying tilt angles of the propeller.

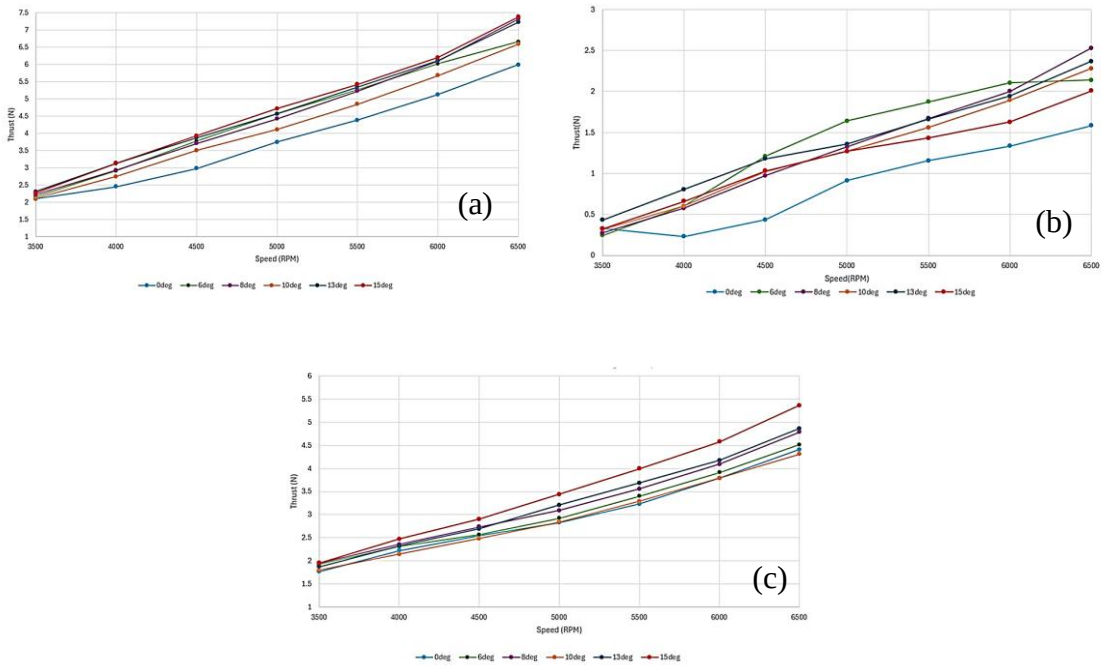

Fig. 15 *(a) Thrust Reading from Load Cell 1*; *(b) Thrust Reading from Load Cell 2; (c) Thrust Difference of Load Cell 1 and 2*

The experimental analysis of coaxial motor-propeller systems revealed that the distance between the propellers and the tilt angle significantly impacts thrust performance differently. Increasing the distance between the propellers from 10 cm to approximately 12 cm initially enhances thrust, likely due to improved aerodynamic interaction. However, as the distance exceeds 12 cm, thrust begins to decline, suggesting that excessive separation reduces the beneficial coupling of the propellers' airflow. On the other hand, adjusting the tilt angle consistently improves thrust across all rotational speeds (RPMs). This effect is attributed to better alignment of airflow and reduced aerodynamic interference between the propellers, especially at higher RPMs where turbulent

interactions are more pronounced. Overall, while both distance and tilt angle adjustments are crucial for optimising thrust, the tilt angle has a more significant and consistent impact on enhancing system performance. Therefore, for practical applications, prioritising the optimisation of the tilt angle is more effective than merely adjusting the distance between propellers. These findings underscore the importance of precise aerodynamic tuning in coaxial motor-propeller systems and suggest that future research should explore the combined effects of both parameters to develop more advanced and efficient propulsion systems tailored to specific operational requirements.

4. Conclusion

This study successfully achieved its goals by designing, fabricating, and testing a test rig for coaxial motor-propeller systems, focusing on the effects of propeller distance and tilt angle on thrust performance. The results indicate that while increasing the distance between the propellers enhances thrust up to an optimal point of around 12 cm, further increases lead to a decline in thrust. In contrast, adjustments to the tilt angle consistently boost thrust across various RPMs, highlighting its critical role in optimising aerodynamic efficiency. Overall, the findings suggest that tilt angle adjustments have a more significant impact on thrust than distance modifications, making them a key factor in improving the performance of coaxial systems. These insights are particularly valuable for enhancing the efficiency of UAVs and eVTOLs, where precise thrust management is crucial.

For practical applications and future research, several recommendations emerge from this study. Firstly, prioritising the fine-tuning of propeller tilt angles is essential, as it offers substantial improvements in thrust and operational performance. Secondly, maintaining an optimal propeller spacing of approximately 12 cm, as identified in this study, is crucial for balancing aerodynamic efficiency and thrust output. Future research should also integrate advanced computational fluid dynamics (CFD) simulations to deepen the understanding of airflow interactions within coaxial systems. Moreover, exploring the combined effects of propeller distance and tilt angle and experimenting with different propeller designs and materials could uncover new ways to maximise thrust and efficiency. Lastly, incorporating these findings into adaptive control systems and applying them to a broader range of aerial vehicles beyond UAVs and eVTOLs could significantly enhance the versatility and performance of coaxial propulsion systems.

Acknowledgement

The authors wish to express their gratitude to the Faculty of Mechanical and Manufacturing Engineering at Universiti Tun Hussein Onn Malaysia for helping to make this study a success.

Conflict of Interest

The authors declare that there is no conflict of interest regarding the publication of the paper.

References

[1] Prasad Rao, J., Holzsager, J. E., Maia, M. M., & Diez, J. F. (2022). Experimental study into optimal configuration and operation of two-four rotor coaxial systems for EVTOL vehicles. Aerospace, 9(8), 452. https://doi.org/10.3390/aerospace9080452

[2] Cerny, M., & Breitsamter, C. (2020). Investigation of small-scale propellers under non-axial inflow conditions. Aerospace Science and Technology, 106, 106048. https://doi.org/10.1016/j.ast.2020.106048

[3] Umar, C. M. I. C., & Zulkafli, M. F. (2021). Distance and Rotational Speed Analysis of Coaxial Rotors for UTHM C-Drone. Progress in Aerospace and Aviation Technology, 1(1), 46-55. https://doi.org/10.30880/paat.2021.01.01.006

[4] Yuan, Y., Chen, R., & Thomson, D. (2020). Propeller design to improve flight dynamics features and performance for coaxial compound helicopters. Aerospace Science and Technology, 106, 106096. https://doi.org/10.1016/j.ast.2020.106096

[5] Villegas, A., Mishkevich, V., Gulak, Y., & Diez, F. J. (2017). Analysis of key elements to evaluate the performance of a multirotor unmanned aerial–aquatic vehicle. Aerospace Science and Technology, 70, 412-418. https://doi.org/10.1016/j.ast.2017.07.046

[6] Raharja, G. B., Gyoubeom, K., & Kwangjoon, Y. (2011). Dynamic Modeling and Control System Design for Coaxial Quadrotor. In Proceedings of International Conference on Intelligent Unmanned Systems (Vol. 7). http://dx.doi.org/10.21535%2FProICIUS.2011.v7.337